Experimental and numerical study of a low-pressure low-frequency Ar-Hg transformer-coupled toroidal discharge

M.V. Isupov, A.V. Fedoseev, G.I. Sukhinin, I.M. Ulanov

Kutateladze institute of thermophysics SB RAS, Novosibirsk, Russia

Low-frequency transformer-coupled toroidal discharge is an electrodeless induction discharge magnetically coupled with inductor by a ferrite core (fig.1). Using ferrite core enhances magnetic coupling, decreases the frequency of induction discharge down to the low frequency range (~10–100 kHz) and increases the power transfer between a power supply and gas discharge. The absence of electrodes significantly increases the life time of gas discharge devices and allows varying the discharge parameters in a very wide range. Thus, new electrodeless UV lamps for UV disinfection and photochemistry with long life-time and high efficiency could be created on the base of the low-frequency Ar–Hg transformer-coupled toroidal discharges [1].

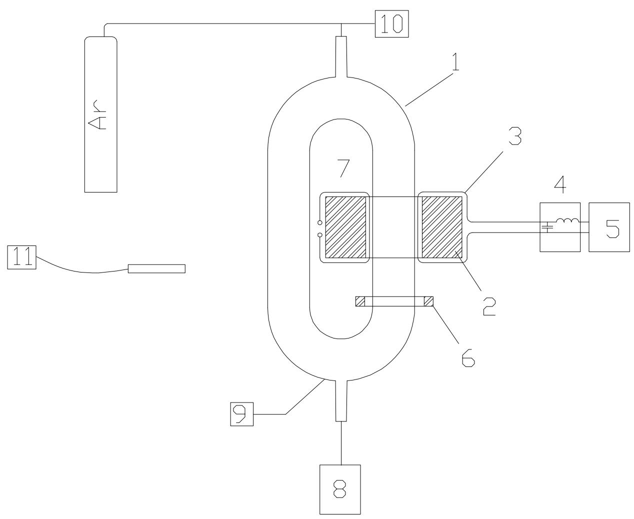

Fig. 1. Experimental setup.

1 – Quartz discharge tube (i.d. 35 мм);

2 – Ferrite core;

3 – Primary winding (inductor);

4 – Matching unit;

5 – Power supply 500 V, 100 kHz;

6 – Current transformer;

7 – A loop of wire;

8 – Fore pump;

9 – Thermocouple;

10 – Vacuum meter;

11 – Spectrometer;

Experiments were performed both with argon flow through the discharge tube *1* and sealed discharge tube filled with a dosed amount of mercury and buffer gas (argon, 100 Pa). To measure discharge current a current transformer *6* was used. To measure discharge voltage a loop of wire *7* enveloping ferrite core *2* was used. The same methods of voltage and current measurements were used in the work [2]. Mercury vapour pressure was determined by the temperature of a cold spot measured with a thermocouple *9*. For spectral measurements an AVASPEC 2048 spectrometer *11* was used allowing measuring the spectral concentration of a radiant flux in the spectral range 200–1100 nm. A special attachment was mounted onto the spectrometer lens to cut out discharge emission in a narrow spatial angle Ω (fig. 2). It allowed to measure spatial profiles of the intensities of mercury lines $I_\lambda(x)$ (fig. 3).

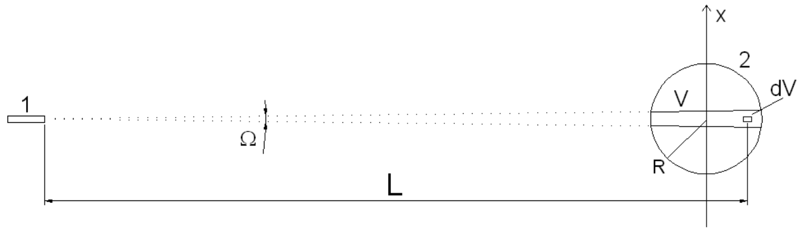

Fig. 2. The method of measuring the spatial profiles of spectral lines.
1 – Photodetector;
2 – Discharge tube.

Spatial profiles of line intensities were calculated with an assumption that radial distributions of line intensities $J_\lambda(r)$ could be described by Bessel function of the first kind of zero order and emission reabsorption was negligible (fig. 3):

$$I_\lambda(x) = \iiint_V \frac{J_\lambda(r)dV}{4\pi L^2} \tag{1}$$

where L is the distance between the spectrometer lens and a voluentary unit dV, V is a volume of gas discharge that emits in the spatial angle Ω, R – discharge tube radius (18 mm). Integration of the equation 1 was performed numerically.

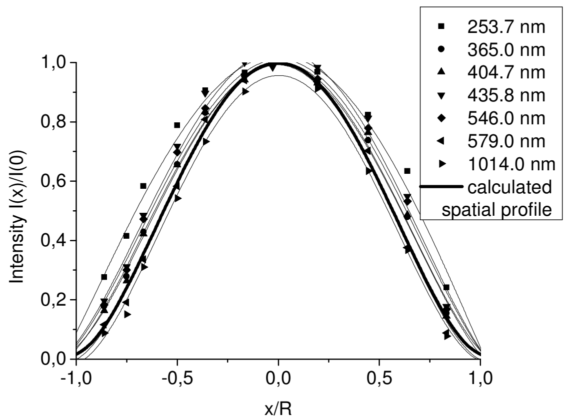

Fig. 3. Spatial profiles of the intensities of mercury lines in the normalized form (discharge current I=3 A, mercury pressure p=1 Pa, argon pressure p=100 Pa).

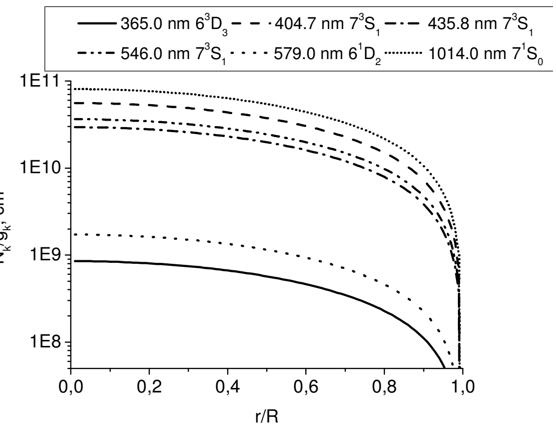

Fig. 4. Radial distribution of the excited atom densities normalized on their statistical weights. I=3 A, p Hg=1 Pa, p Ar=100 Pa.

It is seen in the fig. 3 that the calculated spatial profile coincides indifferently well with experimentally measured spatial profiles of the radiative transitions from 7S, 6D down to 6P excited states of mercury atoms. Spatial profile of the resonant line 253.7 nm is a bit widened probably due to the reabsorption. The coincidence of experimentally measured and calculated spatial profiles of line intensities indicates that mercury excited states have a radial distribution similar to the Bessel function of the first kind of zero order. Using measured intensities of the spectral lines the radial distributions of mercury 7S, 6D excited states were calculated for discharge current 0.5–5 A and mercury vapour pressure 0.5–1.3

Pa (argon pressure was 100 Pa). The calculation for discharge current 3 A and mercury vapour pressure 1 Pa is shown in the fig. 4.

A one-dimensional radial model of the low-frequency transformer-coupled toroidal discharge has been developed based on the assumption of Maxwellian electron energy distribution function. Electron density n_e is described by a balance equation:

$$\frac{\partial n_e(r)}{\partial t} - \frac{1}{r}\frac{\partial}{\partial r}\left(rD_a \frac{\partial n_e(r)}{\partial r} \right) = S_i(r) + S_{sw}(r) + k_{mm} N_m^2(r) - k_{rec} n_e(r) n_i(r) \qquad (2)$$

where S_i is a rate of direct electron impact ionisation, S_{sw} is a rate of stepwise ionisation from the metastable atoms (these values are calculated as integrals of the relevant cross sections), k_{mm} is the rate constant of Penning ionisation as a result of two metastables collision, k_{rec} is the rate constant of radiation recombination in electron-ion collisions, D_a is the electrons and ions ambipolar diffusion coefficient.

Metastable density N_m is described by a balance equation:

$$\frac{\partial N_m}{\partial t} - \frac{1}{r}\frac{\partial}{\partial r}\left(rD_m \frac{\partial N_m}{\partial r} \right) = S_{im}(r) + k_{rec} n_e(r) n_i(r) \\ - k_{em} n_e(r) N_m(r) - 2k_{mm} N_m^2(r) - k_{2B} N_m(r) N_g(r) - k_{3B} N_m(r) N_g^2(r) \qquad (3)$$

where S_{im} is a rate of metastable atoms excitation, k_{em} is the rate constant of stepwise ionisation from metastable atoms calculated by the integration of EEDF with the corresponding cross sections, k_{2B} and k_{3B} are the coefficients of two-body and three-body recombination, D_m is the metastables diffusion coefficient.

The electron energy u_e balance equation has the form:

$$\frac{\partial u_e}{\partial t} + \frac{1}{r}\frac{\partial}{\partial r}\left(r u_e(r) j_r(r) \right) = P_f(r) - P^{el}(r) - \sum_k P_k^{in}(r) + k_{mm} N_m^2(r) \cdot \varepsilon_{mm} \qquad (4)$$

where P_f is the energy gain from the electric field, P^{el} is the energy loss by elastic collisions, P_k^{in} is the energy loss by inelastic collisions. The last term of the eq. 4 describes the energy gain of electrons due to Penning ionization.

Also we take into account gas heating by the electron current and heat conduction to the discharge tube wall. For this purpose we solve the following thermal balance equation:

$$\frac{\partial T_g}{\partial t} - \frac{1}{r}\frac{\partial}{\partial r}\left(r\kappa_g(T_g) \frac{\partial T_g(r)}{\partial r} \right) = P_{el}(r) \qquad (5)$$

where k_g is the heat conductivity coefficient, T_g is the gas temperature. It should be stressed that gas heating strongly influences the discharge characteristics especially under the high gas pressures and discharge currents.

Electrophysical and thermophysical characteristics of the low-pressure argon transformer coupled toroidal discharge have been calculated for argon pressure 10–6000 Pa, discharge current 1–10 A. It is shown that volume recombination overcomes wall recombination at argon pressures higher than 3 Torr leading to the contraction of gas discharge (fig. 5). Also, it is shown that significant (up to 3000 K) gas heating and the relevant gas density decreasing ($N_g(r)=p/kT_g(r)$) results in a dramatic (by an order) falling of the electric field strength E. Experimental investigations of the electrical characteristics of the low-frequency argon transformer-coupled toroidal discharge have been performed that significantly widen the previously studied argon pressure range [2]. Experimental and numerical results are shown in fig. 6.

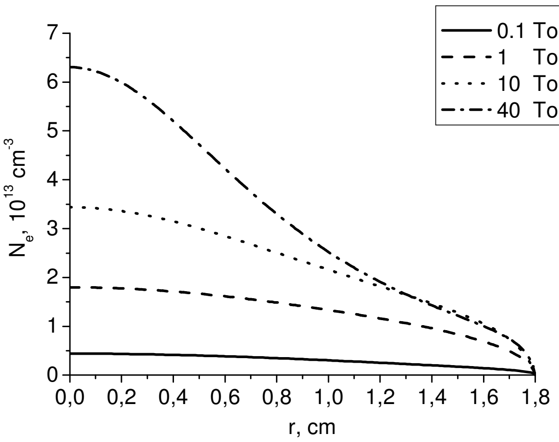

Fig. 5. Radial distribution of electron density for various argon pressures (discharge current 8 A).

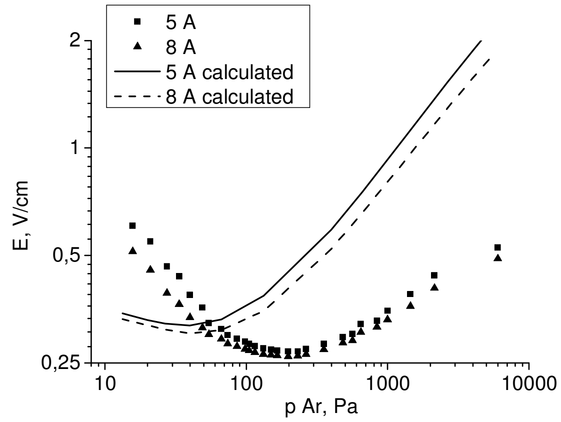

Fig. 6. Electric field strength vs. argon pressure, I = 5, 8 A (numerical and experimental results).

Numerical results describe the key features (the falling voltage-current characteristic and a local minimum of the pressure dependence of electric field strength) of argon transformer-coupled toroidal discharge pretty well. The difference between the numerical and experimental results which is increasing for argon pressures higher than 1 Torr (fig. 6) could be explained by the non-included ionization through higher excited states and dissociative ionization into this tentative model. For example, including the dissociative ionization into the model could increase the contraction effect, leading to the higher gas temperatures on the discharge tube axis, lower gas density and lower electric field strength respectively. We are planning to develop our model and include all these important processes into it. This research was supported by the Russian Foundation for Basic Research, grant number 12-08-00526-a.

1. I. Ulanov, M. Isupov and A. Litvinsev *J. Phys. D.: Appl. Phys.* **40** (2007) 4561.

2. R. Piejak, V. Godyak and B. Alexandrovich *J. Appl. Phys.* **89** (2001) 3590.